

## Tailoring steep density profile with unstable points

Shun Ogawa<sup>1,2</sup> \* Xavier Leoncini<sup>1</sup> † Alexei Vasiliev<sup>3</sup> ‡ and Xavier Garbet<sup>2</sup> §

1. *Aix Marseille Univ., Université Toulon, CNRS, CPT, Marseille, France*

2. *CEA, IRFM, F-13108 St. Paul-lez-Durance cedex, France*

3. *Space Research Institute, Profsoyuznaya 84/32, Moscow 117997, Russia*

The mesoscopic properties of a plasma in a cylindrical magnetic field are investigated from the view point of test-particle dynamics. When the system has enough time and spatial symmetries, a Hamiltonian of a test particle is completely integrable and can be reduced to a single degree of freedom Hamiltonian for each initial state. The reduced Hamiltonian sometimes has unstable fixed points (saddle points) and associated separatrices. Using a maximum entropy principle we compute dynamically compatible equilibrium states of the one particle density function of these systems and discuss how the unstable fixed points affect the density profile or a local pressure gradient, and are able to create a steep profile that improves plasma confinement.

Being able to sustain a steep density profile in hot magnetized plasma is one of the major key points to achieve magnetically confined fusion devices. These steep profiles are typically associated with the emergence in the plasma of so-called internal transport barriers (ITB) [1, 2]. Both the creation and study of these barriers have generated numerous investigations mostly numerical using either a fluid, or magnetic field or kinetic perspective or combining some of these. In this paper starting from the direct study of particle motion, we propose a simple mechanism to set up a steep profile which may not have been fully considered yet. Indeed, charged particle motion in a non-uniform magnetic field [3–9] is one of main classical issues of physics of plasmas in space or in fusion reactors. To tackle this problem the guiding center [7] and the gyrokinetic [8] theories are developed to trace the particle's slower motion by averaging the faster cyclotron motion. These reductions suppress computational cost and they are widely used to simulate the magnetically confined plasmas in fusion reactors [6]. These reduction theories assume existence of an invariant or an adiabatic invariant of motion associated with the magnetic moment. Meanwhile, this assumption does not always hold true. Then, recently, studies on full particle orbits without any reductions are done to look into phenomena ignored by these reductions and to interpolate the guiding center orbit. There exists a case that a guiding center trajectory and a full trajectory are completely different [10]. Further, it is found that the assumption of the invariant magnetic moment breaks [11, 12] due to the chaotic motion of the test particles.

Let us quickly review the single particle motion and adiabatic chaos. We consider a model of charged particle moving in a non-uniform cylindrical magnetic field  $\mathbf{B}(r) = \nabla \wedge \mathbf{A}_0(r)$ . The vector potential  $\mathbf{A}_0(r)$  is given by

$$\mathbf{A}_0(r) = \frac{B_0 r}{2} \mathbf{e}_\theta - B_0 F(r) \mathbf{e}_z, \quad F(r) = \int_0^r \frac{r dr}{R_{\text{per}} q(r)}, \quad (1)$$

where the cylinder is parametrized with the coordinate  $(r, \theta, z)$ ,  $B_0$  is strength of the magnetic field,  $z$  has  $2\pi R_{\text{per}}$  periodicity,  $\mathbf{e}_\theta$  and  $\mathbf{e}_z$  are basic units for each direction, and

$q(r)$  is a winding number called a safety factor of magnetic field lines. The Hamiltonian of the particle  $H = \|\mathbf{v}\|^2/2$ , where  $\mathbf{v}$  denotes particle's velocity, has three constants of motion, the energy, the angular momentum, and the momentum, associated with time, rotational, and translational symmetry of the system respectively, so that the Hamiltonian  $H$  on the six dimensional phase space is reduced into the single-degree-of-freedom Hamiltonian on the two dimensional phase space,  $(r, p_r)$ -plane [11, 12],

$$H_{\text{eff}}(r, p_r) = p_r^2/2 + V_{\text{eff}}(r),$$

$$V_{\text{eff}}(r) = \frac{v_\theta^2 + v_z^2}{2} = \frac{(p_\theta^2 r^{-1} - B_0 r/2)^2}{2} + \frac{(p_z + B_0 F(r))^2}{2}. \quad (2)$$

where  $p_i$  stands for the conjugate momentum for  $i = r, z$ , and  $\theta$  respectively, and where  $v_\theta = r\dot{\theta}$  and  $v_z = \dot{z}$ . The upper dot denotes  $d/dt$ . Invariants  $p_z$  and  $p_\theta$  are fixed by an initial condition. Appropriately setting the safety factor  $q$  and choosing initial condition, we can find an unstable fixed point in  $(r, p_r)$  phase plane, which can induce the adiabatic chaos [13–17] when the weak magnetic perturbation or the curvature effect added to the flat torus (cylinder) exist[11, 12].

This Letter aims to exhibit one possibility that the unstable fixed point inducing chaotic motion modifies mesoscopic properties of plasmas, local density and pressure gradients which are believed to be associated with the internal transport barriers (ITBs) [1, 2] a feature missed by gyrokinetics, or a pure magneto-hydrodynamic approach.

For this purpose, this Letter deals with the radial density function  $\rho(r)$  derived from the maximal entropy principle, which is a steady state of a truncated Vlasov-Maxwell system with an ion moving in a static magnetic field. We qualitatively discuss which kind of vector potentials  $F(r)$  or  $q$ -profiles are likely to bring about the unstable fixed point for the test particle motion. Then, we look into the effect of the unstable fixed point for the density profile and the local-pressure gradient. We shall end this Letter by remarking the relation between the steep density profile (particle's ITBs) and the magnetic ITBs [18, 19].

Let us now compute the density profile. The Vlasov-

Maxwell system consists of the collisionless Boltzmann equation describing a temporal evolution of single particle density functions of ions and electrons, coupled with the Maxwell equation determining a self-consistent electromagnetic field [20, 21]. Before dealing with such a very complex system, it is worthwhile to consider the test particle motion in static nonuniform magnetic fields. We neglect electrons (their presence insures a neutralizing background, and the current to get the right poloidal component of magnetic field), inter-particle interactions, radiation from moving charged particles and back reaction from the electromagnetic field. The Boltzmann's constant  $k_B$  is set as unity. Let us consider a steady state associated with a density function  $f_0$  on the phase space, which commutes with Hamiltonian (2). There exist infinitely many steady states, but assuming a vanishing collisionality, we may consider that the one maximizing the information entropy under suitable constraint conditions is picked out [22, 23]. Thus  $f_0$  maximizes the information entropy (also called a density of the Boltzmann Gibbs entropy)

$$\mathcal{S}[f] = - \iint_{\mu} f \ln f d^3 \mathbf{p} d^3 \mathbf{q}, \quad (3)$$

subject to the normalization condition and energy, momentum, and angular momentum conservations, which are respectively

$$\begin{aligned} \mathcal{N}[f] &= \iint_{\mu} f d^3 \mathbf{p} d^3 \mathbf{q}, & \mathcal{E}[f] &= \iint_{\mu} H_{\text{eff}} f d^3 \mathbf{p} d^3 \mathbf{q}, \\ \mathcal{P}[f] &= \iint_{\mu} p_z f d^3 \mathbf{p} d^3 \mathbf{q}, & \mathcal{L}[f] &= \iint_{\mu} p_{\theta} f d^3 \mathbf{p} d^3 \mathbf{q}, \end{aligned} \quad (4)$$

where the integral  $\iint_{\mu} \bullet d^3 \mathbf{p} d^3 \mathbf{q}$  means average over the six dimensional single particle phase space, noted here  $\mu$ -space. The solution to this variational problem is

$$f_0 = e^{-\beta H_{\text{eff}} - \gamma_1 - \gamma_{\theta} p_{\theta} - \gamma_z p_z} \quad (5)$$

where  $\beta$ ,  $\gamma_1$ ,  $\gamma_{\theta}$ , and  $\gamma_z$  are the Lagrangian multipliers, associated with energy conservation, normalization, momentum and angular momentum conditions respectively. The parameter  $\beta$  corresponds to the thermodynamical temperature as  $T_{\text{th}}^{-1} \equiv \beta = \delta \mathcal{S} / \delta \mathcal{E}$ , and it can be safely assumed positive. It should be noted that  $-\gamma_{\theta}$  and  $-\gamma_z$  are proportional to the ensemble averages of  $v_{\theta}$  and  $v_z$  respectively. In the literature is has been admitted that when an ITB exists plasma rotation exists. We then expect that in such state the averages of  $v_{\theta}$  and  $v_z$  are not 0 and so are  $\gamma_{\theta}$  and  $\gamma_z$ , which are negative. The spatial density function  $n(\mathbf{q})$  is deduced from this result as

$$n(\mathbf{q}) \equiv \int f_0 d^3 \mathbf{p} = \int f_0 r^{-1} d p_{\theta} d p_z d p_r. \quad (6)$$

Thus, the density  $n(r) d^3 \mathbf{q}$  is proportional to

$$n(\mathbf{q}) r dr d\theta dz \propto e^{\left( \frac{\gamma_{\theta}}{2} \left( -B_0 - \frac{\gamma_{\theta}}{\beta} \right) r^2 + \gamma_z B_0 F(r) \right)} r dr d\theta dz, \quad (7)$$

and is independent of  $\theta$  and  $z$ . We then obtain a radial density function  $\rho(r)$  given by

$$\rho(r) = \frac{\iint n(\mathbf{q}) r dr d\theta dz}{\iint r dr d\theta dz} = \frac{1}{4\pi^2 r R_{\text{per}}} \iint n(\mathbf{q}) r dr d\theta dz, \quad (8)$$

as

$$\begin{aligned} \rho(r) &= \frac{\exp(-ar^2 - bF(r))}{\int_0^1 \exp(-ar^2 - bF(r)) dr}, \\ a &= -\frac{\gamma_{\theta}}{2} \left( -B_0 - \frac{\gamma_{\theta}}{\beta} \right), \quad b = -\gamma_z B_0. \end{aligned} \quad (9)$$

It should be noted that the local pressure  $P(r)$  is proportional to the radial density  $\rho(r)$ , because we assume the equation of state  $P(r) = N\rho(r)T_{\text{th}}$  holds locally true, where  $N$  is the number of particles.

We now move on and consider how the existence of the unstable fixed points with relevant energy level affects the obtained equilibrium density profile. For this purpose we have to discuss how the safety factor is chosen, in other words which function  $F$  in Eq. (1) leads to the emergence of "practical" unstable points in the effective potential  $V_{\text{eff}}$ . Indeed, as a first point to pin out, if the amplitude of  $F$  is large, we can expect that the term  $v_z^2/2 = (p_z + F)^2/2$  in the Hamiltonian (2) becomes also large, then the unstable points appear in the phase space at so high energy level that they become physically irrelevant. Therefore, the amplitude of  $F$  should be small.

Moreover if the variations of  $F(r)$  are smooth and "gentle" with  $r$ , so does again  $(p_z + F)^2/2$  in  $V_{\text{eff}}$ , then  $V_{\text{eff}}$  has only one minimum point that is essentially governed by the term  $(p_{\theta}/r - B_0 r/2)^2/2$ . Thus, enough concavity of  $v_z^2/2$  near but not at the minimum point of  $(p_{\theta}/r - B_0 r/2)^2/2$ ,  $r = \sqrt{2p_{\theta}/B_0}$  is necessary so that  $V_{\text{eff}}$  has unstable points. These considerations are illustrated in Fig. 1. In the panel (d), we assume that there exists an  $r$  such that  $p_z + F(r) = 0$ . We stress out as well that if  $|p_z|$  is sufficiently large, it is also possible to create an unstable point, but then again the energy level is so high that it is irrelevant for the mesoscopic profiles in considered plasmas.

Since the safety factor  $q(r)$  can be directly associated with the function  $F(r)$  at the origin of the unstable fixed points, and  $q(r)$  is a crucial parameter for the operation of magnetized fusion machine, let us discuss more how the constraints discussed previously translate on the  $q$ -profile. For instance let us consider a situation with a non-monotonous profile such that  $q(r)$  has a minimum  $q_0$  at  $r = \alpha$  and the spatial scale is characterized with  $\lambda$ . Then locally  $q(r)$  can be expressed as

$$q(r) = q_0 [1 + \lambda^2 (r - \alpha)^2], \quad r \sim \alpha. \quad (10)$$

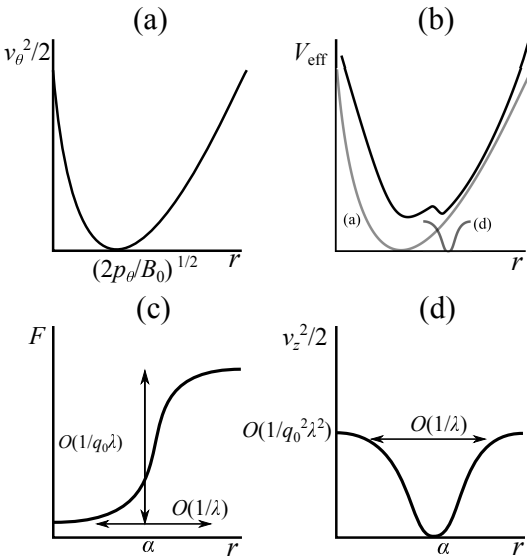


FIG. 1. Schematic picture showing how the saddle point appears around the bottom of safety factors. A Panel (a) represents a part of  $v_\theta^2/2 = (p_\theta/r - B_0 r/2)^2/2$ , (b)  $V_{\text{eff}}$ , (c)  $F(r)$ , and (d)  $v_z^2/2 = (p_z + F(r))^2/2$ . In the panel (d), we consider that there exists an  $r$  such that  $p_z + F(r) = 0$ . The parameters  $q_0$ ,  $\lambda$ , and  $\alpha$  are associated with Eq. (10).

Recalling Eq. (1), the function  $F$  is scaled as  $q_0^{-1}\lambda^{-1}$ , and  $v_z^2/2 = (p_z + F)^2/2 \sim q_0^{-2}\lambda^{-2}$ , so that this provides a typical energy level of the particles located near a separatrix. It should be noted that the width of the well of  $v_z^2/2$  scales as  $\lambda^{-1}$  (see Fig. 1). For a fixed value of  $q_0$ , a large value of  $\lambda$  creates unstable fixed points with relevant energy levels for the particle whose angular momentum is  $p_\theta \sim B_0\alpha^2/2$ . As  $\lambda$  gets to be larger, the number of the particles with unstable fixed point increase. This is because, roughly speaking, the energy levels of unstable points get to be lower, and the one-particle density (5) is proportional to  $e^{-\beta H_{\text{eff}}}$ . As a consequence of these considerations we illustrate on Fig. 2 how to adjust a given  $q$ -profile in order to create unstable fixed points whose location is  $r \sim \alpha$ . One can set up unstable fixed point around  $r \sim \alpha$  by modifying the  $q$ -profile so that it has concavity around  $r = \alpha$ .

We then have a form of density profile (9) and a condition for  $q$ -profile exhibiting unstable fixed points. We next consider where the unstable points appear, and we shall exhibit that the emergence of unstable fixed points induces the presence of a local steep profile in their vicinity, *i.e.* their radial positions are inducing the existence of locally strong density gradients. For this purpose we simply consider the  $q$ -profile given by Eq. (10) with parameters  $q_0 = 0.12$ ,  $\lambda = 55$ , and  $\alpha = \sqrt{0.18} \approx 0.4243$ , in Figs. 3 and 4. When including perturbations, we point out that the adiabatic chaos due to separatrix crossing in this magnetic field has been discussed in Ref. [11]. The results are displayed in Fig. 3, where two density profiles (9) obtained for two  $q$ -profiles with and without unstable fixed points are shown. The parameter  $a$

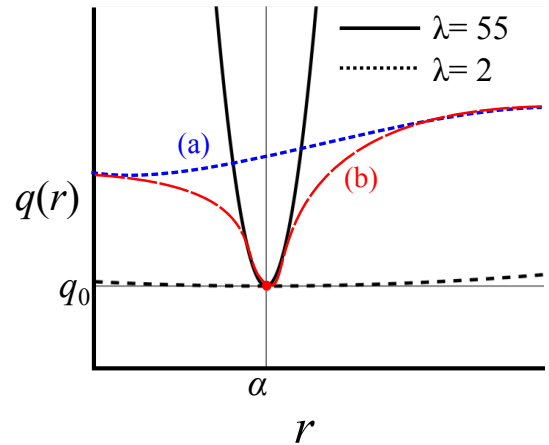


FIG. 2. Schematic picture exhibiting how to create unstable fixed point by modifying  $q$ -profile. The solid curve represents the given  $q$ -profile. Dotted and bold curves are the graph of  $q_0(1+\lambda^2(r-\alpha)^2)$  for  $q_0 = 0.12$ ,  $\alpha = \sqrt{0.18}$  and  $\lambda = 2, 55$  respectively. The  $q(r)$  with  $\lambda = 55$  induces the unstable fixed points, so does not one with  $\lambda = 2$ . (a) and (b) correspond respectively to the  $q$ -profiles without and with unstable fixed points.

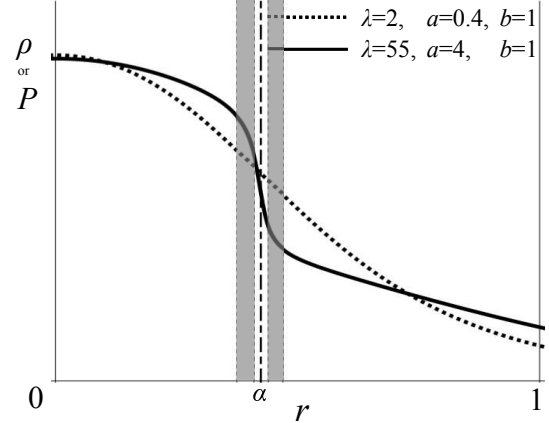


FIG. 3. (Color online) The solid and dotted curves express the density profiles with  $q$ -profiles with unstable points (shaded region) and without unstable points respectively. The parameters in a local  $q$ -profile [Eq. (10)] are determined as  $q_0 = 0.12$ , and  $\alpha = \sqrt{0.18} \approx 0.4243$ , and  $\lambda = 55$  for the solid curve and  $\lambda = 2$  for the dotted one. In both profiles,  $\gamma_z$  and  $\beta$  are same, but  $\gamma_\theta$  is different.

is changed so that they have same density in the center of cylinder. We note  $a$  can be changed keeping the thermodynamical temperature  $\beta^{-1}$  and changing the average of angle velocity  $v_\theta$ . We find the steep region which corresponds to the local steep density gradient around  $r = \alpha$  on which  $q(r)$  satisfies  $q'(r) = 0$  for the  $q$ -profile with unstable points. In Fig. 4, we exhibit the locations of unstable fixed points and their energy levels. We can notice that the unstable fixed points appear in  $r \approx \alpha$  but not exactly on  $r = \alpha$ .

Before concluding this letter we would like to make some remarks on the observed profiles which indicate the presence of what we may call an ITB although the underlying

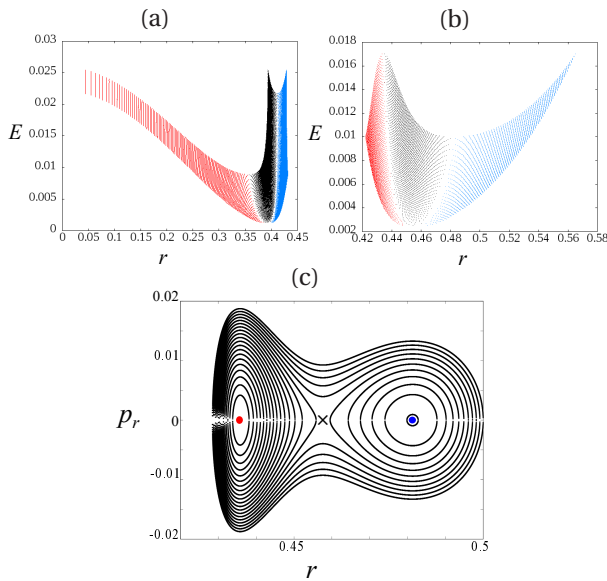


FIG. 4. (Color online) Panels (a) and (b) are for place and energy levels of the saddle points in the inside and outside of the magnetic ITB respectively. Panel (c) shows the iso- $H_{\text{eff}}$  contours, a saddle point (black  $\times$ ), and elliptic points (blue and red points). The parameters in a local  $q$ -profile [Eq. (10)] are determined as  $q_0 = 0.12$ ,  $\lambda = 55$ ,  $\alpha = \sqrt{0.18} \simeq 0.4243$ . In Panels (a) and (b), black dotted region (center) represents a set of saddle points and the blue (right) and red (left) ones represent sets of elliptic points respectively, and their colors are corresponding to the ones in Panel (c). The energy  $E$  is given by the energy at saddle point for each effective Hamiltonian.

physical mechanisms are quite different. We would like to stress out the similarities and differences between our observations and the magnetic ITBs discussed for instance in [19]. One of the main difference is that if the plateau of  $q(r)$  appears the transport barrier appears even if the value of  $q$  is far from rational number  $m/n$  with small integers  $m$  and  $n$ , meaning the existence of this barrier does not appear to be correlated to the existence of a resonant surface, on the other hand in the considered example, the location of the magnetic ITB coincides with the place on which the local density gradient exists.

Another study between the particle's motion and the existence of an ITB using a pure field line approach and the existence of a stable magnetic tori has been performed from the view point of the difference between the magnetic winding number  $q(r)$  and the effective one  $q_{\text{eff}}(r)$  for the guiding venter orbit of the energetic particles [24]. In a recent study [25], it is shown that the resonance shift due to the grad  $B$  drift and its disappearance due to the curvature drift effect can create an invariant tori in the particle dynamics while there are none for magnetic field lines, and this is confirmed both analytically and numerically with the full particle orbits around the resonance points. It should be remarked that the guiding center theory is useless to clarify it unlike Ref. [25].

The above consideration provides de facto another difference between the magnetic ITB and the effective ITB induced by the separatrices. Moreover, we can stress out that the magnetic ITB is present in both situations described in Fig. 3, while the steep profile occurs only when the hyperbolic points are present. We also note that the two unstable fixed points appear around the magnetic ITB and when the parameter  $\lambda$  in Eq. (10) gets to be large, the steep region of  $\rho(r)$  gets to be strong as the influence of the separatrix grows because the gap of  $F(r)$  between  $r < \alpha$  and  $r > \alpha$  becomes smaller (see Fig. 1), and this explains why we obtain a local steepness of the density and the local pressure gradient around the magnetic ITB. To conclude, we have shown in this letter that steep equilibrium density profiles can emerge due to the presence of a separatrix in the passive particle orbits, this phenomenon is not related to the existence of a local resonant surface and the observed phenomenon is reminiscent of the presence of an ITB although the physical mechanisms inducing it are a priori quite different in interpretation. We also discussed how the  $q$ -profile can be tuned in order to generate such barriers.

We finally remark on what happens if we consider a toroidal configuration. Let us imagine our cylindrical system is an infinite toroidal radius limit of the toroidal system as Ref. [12]. The finite toroidal radius effect breaks the integrability and it thus can induces adiabatic chaos. It has been known for a while that the presence of chaos affects sometimes the density profile locally. For instance, the averaging effect in plasmas from the global chaos induced by the resonance overlapping [26] has been found and it modifies the density profile [27]. Even though we are directly tackling the passive particle motions of ions and thus a different type of localized chaos in this letter, similar things can be expected. In the present case the unstable fixed points are located around the place in which the steepness of density (9) and the local pressure gradient exist as shown in Figs. 3 and 4. Therefore the flattening effect makes them steeper locally. As a result we can expect that this steepening effect observed in the cylindrical configuration can be robust at least as long as strongly chaotic motion remains localized near each hyperbolic point.

S. O. and X. L. thank G. Dif-Pradalier for useful and encouraging discussions. This work has been carried out within the framework of the French Research Federation for Magnetic Fusion Studies. We acknowledge the financial support of the A\*MIDEX project (n°ANR-11-IDEX-0001-02) funded by the “investissements d’Avenir” French Government program, managed by the French National Research Agency (ANR).

\* shun.ogawa@cpt.univ-mrs.fr

† xavier.leoncini@cpt.univ-mrs.fr

‡ valex@iki.rssi.ru

§ xavier.garbet@cea.fr

- [1] R. C. Wolf, Internal transport barriers in tokamak plasmas, *Plasma Phys. Control. Fusion* **45**, R1 (2003).
- [2] J. W. Connor, T. Fukuda, X. Garbet, C. Gormezano, V. Mukhovatov, M. Wakatani, ITB Database Group, and ITPA Topical Group on Transport and Internal Barrier Physics, A review of internal transport barrier physics for steady-state operation of tokamaks, *Nucl. Fusion* **44**, R1 (2004).
- [3] H. Alfvén, On the motion of a charged particle in a magnetic field, *Ark. Mat. Astron. Fys.* **27A**, 1 (1940); *Cosmological electrodynamics*, (Oxford university press, London, 1950).
- [4] T. G. Northrop, The guiding center approximation to charged particle motion, *Ann. Phys.* **15**, 79 (1961).
- [5] R. G. Littlejohn, Hamiltonian formulation of guiding center motion, *Phys. Fluids* **24**, 1730 (1981).
- [6] A. H. Boozer, Physics of magnetically confined plasmas, *Rev. Mod. Phys.* **76**, 1071 (2004).
- [7] J. R. Cary and A. J. Brizard, Hamiltonian theory of guiding-center motion, *Rev. Mod. Phys.* **81**, 693 (2009).
- [8] A. J. Brizard and T. S. Hahm, Foundations of nonlinear gyrokinetic theory, *Rev. Mod. Phys.*, **79**, 421 (2007).
- [9] J. D. Jackson, *Classical Electrodynamics*, 3rd ed. (Wiley, USA, 1998).
- [10] D. Pfefferl  , J. P. Graves, and W. A. Cooper, Hybrid guiding-centre/full-orbit simulations in non-axisymmetric magnetic geometry exploiting general criterion for guiding-centre accuracy, *Plasma Phys. Controlled Fusion* **57**, 054017 (2015).
- [11] S. Ogawa, B. Cambon, X. Leoncini, M. Vittot, D. del-Castillo-Negrete, G. Dif-Pradalier, and X. Garbet, Full particle orbit effects in regular and stochastic magnetic fields, *Phys. Plasmas* **23**, 072506 (2016).
- [12] B. Cambon, X. Leoncini, M. Vittot, R. Dumont, and X. Garbet, Chaotic motion of charged particles in toroidal magnetic configurations, *Chaos* **24**, 033101 (2014).
- [13] A. I. Neishtadt, Change of an adiabatic invariant at a separatrix, *Sov. J. Plasma Phys.* **12**, 568 (1986).
- [14] A. I. Neishtadt, On the change in the adiabatic invariant on crossing a separatrix in systems with two degrees of freedom, *Prikl. Matem. Mekhan. USSR* **51**, 586 (1987).
- [15] J. L. Tennyson, J. R. Cary, and D. F. Escande, Change of the adiabatic invariant due to separatrix crossing, *Phys. Rev. Lett.* **56**, 2117 (1986).
- [16] J. R. Cary, D. F. Escande, and J. L. Tennyson, Adiabatic-invariant change due to separatrix crossing *Phys. Rev. A* **34**, 4256 (1986).
- [17] X. Leoncini, A. Neishtadt, and A. Vasiliev, Directed transport in a spatially periodic harmonic potential under periodic nonbiased forcing, *Phys. Rev. E* **79**, 026213 (2009).
- [18] R. Balescu, Hamiltonian nontwist map for magnetic field lines with locally reversed shear in toroidal geometry, *Phys. Rev. E* **58**, 3781 (1998).
- [19] D. Constantinescu and M.-C. Firpo, Modifying locally the safety profile to improve the confinement of magnetic field lines in tokamak plasmas *Nucl. Fusion* **52**, 054006 (2012).
- [20] A. A. Vlasov, The vibrational properties of an electron gas, *Zh. Eksp. Ther. Fiz.* **8**, 291 (1938); *Sov. Phys. Uspekhi* **93** (1968).
- [21] L. P. Pitaevskii and E.M. Lifshitz, *Physical Kinetics* (Butterworth-Heinemann, Oxford, 1981)
- [22] T. M. Rocha Filho, A. Figueiredo, and M A. Amato, Entropy of classical systems with long-range interactions, *Phys. Rev. Lett.* **95**, 190601, (2005).
- [23] D. Zubarev, V. Morozov, and G. R  pke, *Statistical Mechanics of Nonequilibrium Processes, Volume 1: Basic concepts, kinetic theory* (Academic Verlag, Berlin, 1996).
- [24] G. Fiksel, B. Hudson, D. J. Den Hartog, R. M. Magee, R. O'Connell, and S. C. Prager, Observation of weak impact of a stochastic magnetic field on fast-ion confinement, *Phys. Rev. Lett.* **95**, 125001 (2005).
- [25] S. Ogawa, X. Leoncini, G. Dif-Pradalier, and X. Garbet, Study on creation and destruction of transport barriers via effective safety factors for energetic particles, arXiv:1610.02867, (to appear in *Phys. Plasmas*).
- [26] B. V. Chirikov, A universal instability of many-dimensional oscillator systems, *Phys. Rep.* **52**, 263 (1979).
- [27] R.B. White, Modification of particle distributions by MHD instabilities I, *Commun. Nonlinear Sci. Numer. Simulat.* **17**, 2200 (2012); Modification of particle distributions by MHD instabilities II, *Plasma Phys. Control. Fusion* **53**, 085018 (2011).